A New Method to Understand the IR Spectra of the HCl-Water Clusters

Rui-Jie Xue,[†] Zexing Qu,[†] Hui Li,[*,†] and Jiali Gao[*,†,‡]

[†]Institute of Theoretical Chemistry, State Key Laboratory of Theoretical and Computational Chemistry, Jilin University, 2519 Jiefang Road, Changchun 130023, People's Republic of China

[‡]Department of Chemistry and Supercomputing Institute, University of Minnesota, Minneapolis, Minnesota 55455

Supporting Information Placeholder

ABSTRACT: We reproduce the experimental spectrum of the HCl-water clusters by a new method. The method is the combination of quantum mechanics and classical mechanics to deal with the nucleus motion. The stretching vibrational mode of the chromophore molecule HCl is treated in quantum mechanics and the other degrees of freedom (DOFs) are sampled from classical molecular dynamics simulations. Based on one-order of perturbation theory, time dependent band origin shifts are obtained and applied to study linear and two-dimensional (2D) pump-probe vibrational spectra. The calculated vibrational frequency of the HCl stretching mode in $HCl(H_2O)_1$ cluster is only 12.8 cm^{-1} away from the experimental value, which is nearly 16 times (190.72 cm^{-1}) improvement compared with the results obtained from the traditional method, and the predicted spectroscopic line shape is also consistent with the experimental result. In addition, the method can also be used to explore the relaxation process of the coupling of resonance bands between 1-0 resonance and 2-1 resonance of the HCl stretching vibrational mode. The decoupling process is traced by the 2D pump-probe spectra if we change the evolution time.

1. INTRODUCTION

The microscopic behaviors of the HCl-water clusters have led some fundamental subjects of physical and chemical processes, including ozone-destroying chain reactions[1-7] and Brønsted acid/base dissociation.[8-15] Understanding the IR spectra of the HCl-water clusters is the effective way to investigate the microscopic behaviors of the HCl-water clusters including the structural variation and the dynamical processes, such as the process of HCl dissociation. Due to such a fundamental importance of the HCl-water clusters, they have attracted enormous studies in both experiments[16-24] and theories.[1,8-13,15,25-44]

Suhm *et al.* [16,17]reported the first experimental IR spectrum of HCl-water clusters twelve years ago and assigned the acidic proton vibration of undissociated clusters $(HCl)_2(H_2O)_1$ and $HCl(H_2O)_n$ (n=1,2), but failed to assign the $HCl(H_2O)_3$ cluster due to the low concentration of the cluster in the gas expansion.[17] This unmeasured vibrational band

is discussed in the result part of this paper. Another recent experimental work given by Havenith and co-workers confirmed that the broad band at 2675 cm^{-1} contains "dissociated clusters formed by the aggregation of four H_2O and one HCl molecules being the smallest dissociated cluster i.e. the smallest droplet of acid" .[24]

In theoretical works, Bowman *et al.*[40,43] employed the Diffusion Monte Carlo simulation to investigate the HCl stretching vibration which has a delocalized zero-point vibrational motion in the $HCl(H_2O)_2$ cluster. The vibrational frequency based on the semiempirical and high-level ab initio potential[40] has a good agreement with the experimental value. But no spectroscopic line shape is reported in their works. Ab initio molecular dynamics (AIMD) simulations with DFT-base potential have obtained enormous successes to investigate the properties of $HCl(H_2O)_n$ (n=1,2,3,4) clusters.[12,26,34,35] Dominik *et al.*[26] used the Fourier transform of the dipole autocorrelation function (DAF) to obtain the IR spectra of the HCl-water clusters which are based on AIMD simulations. They also demonstrated the start point of HCl dissociation in growing n up to 4 and the smallest dissociated structure is determined by the interplay of both quantum and thermal fluctuation.[9,13,26,29,30]

The first step of understanding such an IR spectrum is to reproduce the experimental spectrum accurately. The main challenges of the precise description of the IR spectra can be summarized as: 1) the construction of the intra- and intermolecular force field in the system including hydrogen-bonds, 2) how to include the quantum effect of the specific vibrational mode of the complexes whose configurations are sampled from classical molecular dynamics simulations, 3) the precise description of the anharmonic contribution and the relaxation process of the coupling between different vibrational modes, and 4) the separation of the specific vibrational mode from the flexible hydrogen-bonding network.

The new method has overcome the above deficiencies. Our method is to abstract the HCl stretching vibrational mode and describe it as wave functions. The DOFs of the intermolecular interaction are treated classically and they are regarded as the variables of the perturbation term. In fact, the theoretical spectroscopic position of the $HCl(H_2O)_1$ cluster which is calculated by the new method with the potential of CCSD(T)-F12b[45]/cc-pVTZ-F12 is only 12.8 cm^{-1} away from the experimental value, which is nearly 16 times improvement comparing with the DAF method. The results of other sizes of the clusters, based on the potential calculation of the functional M06-2x,[46] are also in good agreements with the experimental values and will be discussed in the result part. In addition, due to the structural flexibility and fluctuations of the hydrogen-bonded system, the coupling may be happened between different resonance states. Thus, it has the great significance to add the second dimension to the 1D IR spectra to explore the comprehensive evolution of the two coupling resonances.[25,47-49] The pump-probe 2D spectra will be discussed in the results part. At last, the smallest size of the dissociation structure of the cluster is also discussed in this work.

This paper is organized as follows. In section 2, the methods of the calculation of transition frequency, linear spectra, two-dimensional spectra and the computational details are described. The results are discussed in section 3. The conclusions are then devoted in section 4.

2. Method

2.1. Calculation of transition frequency. A chromophore molecule of hydrogen chloride (HCl)

is embedded into the hydrogen bonding network formed by water and other HCl molecules. In order to obtain the transition frequency of HCl stretching vibration in the complex, We make an assumption that the HCl stretching vibrational mode can have an adiabatic separation from other DOFs due to HCl stretching vibrational mode is orders of magnitude faster than other relative intermolecular motions.[50,51] We employ the one-order perturbation theory, and the intermolecular interactions between the HCl and other molecules are regarded as the perturbation term in the Hamiltonian of the chromophore molecule in complex system. Thus, the Hamiltonian is given as

$$H_{\text{cluster}} = H_0 + \Delta V(R, Q) \qquad (1)$$

Where H_0 is the Hamiltonian of a free HCl molecule, and the Q , R represent the intramolecular and intermolecular coordinate sets, respectively. The wave function can be separated into intramolecular and intermolecular part as

$$\psi(Q, R) = \phi(R)\varphi(Q) \qquad (2)$$

due to the adiabatic approximation. The H_0 is given as

$$H_0 = T + V_{\text{HCl}}(Q) \qquad (3)$$

Then we give the 1D time-independent Schrödinger equation as

$$T\,|\,\varphi_\upsilon\rangle + V_{\text{HCl}}(Q)\,|\,\varphi_\upsilon\rangle = E^\upsilon\,|\,\varphi_\upsilon\rangle \qquad (4)$$

The potential optimized discrete variable representation (PODVR)[52,53] grids are used for the HCl stretching vibrational mode of the 1D Schrödinger equation with a precise potential curve and the potential curve is obtained based on the experimental data.[54] After numerous tests, 5 grids are fine enough to depict the wave functions of the HCl stretching vibrarional states, thus this stretching vibrational wave function is given approximately as

$$|\,\varphi_\upsilon\rangle = \sum_{i=1}^{5} c_{\upsilon i}\,|\,\chi_{Q_i}\rangle \qquad (5)$$

Where υ =1, 2, 3... represent vibrational ground state, first excited state, second excited state... The wave functions are illustrated in Figure 1. The remarkable reduction in computational effort is attained if the one order perturbation approximation is applied into the calculation of the frequency shifts.[50,51,55-60] The perturbation term is expressed as

$$\begin{aligned}\Delta V^\upsilon &= \int dQdR\phi^*(R)\varphi_\upsilon^*(Q)\Delta V(R,Q)\varphi_\upsilon(Q)\phi(R)\\ &= \sum_R\sum_i^5 \phi^*(R)c_{\upsilon i}^*\Delta V(R,Q_i)c_{\upsilon i}\phi\ (R)\\ &= \sum_R \Delta V^\upsilon(R)\rho(R) \qquad (6)\end{aligned}$$

the equ. (6) representing the calculation of the shift of the energy level can be divided into two steps. The first step is regarded as the average of intramolecular coordinates (the sum of intramolecular PODVR grids) and the second step is thought as the average of the intermolecular coordinates. The process of the frequency shift is illustrated in figure 2. The average of transition frequency between υ =1 and υ =0 is given as

$$\overline{\omega}_{10} = 2\pi\cdot(\Delta V^{\upsilon=1} + \Delta V^{\upsilon=0} + \Delta E_{\text{free}}^{10})/h \qquad (7)$$

The potential energy was calculated in two level electronic structure method：the functional BLYP with the plane wave basis set and the functional M06-2x with the basis set of cc-pVTZ; the higher level method CCSD(T)-F12 with the cc-pVTZ-F12 basis set in which the basis set superposition error (BSSE) had been considered in our calculation. The results will be discussed in the section of RESULTS AND DISCUSS.

2.2. Calculation of linear spectra. In traditional way, the spectroscopic line shape is given via the Fourier transform of the DAF

$$I(\omega) \sim \int_0^\infty dt e^{-i\omega t} \langle \mu(0) \cdot \mu(t) \rangle \quad (8)$$

Where $\mu(0)$ and $\mu(t)$ are the dipole moments at the time 0 and t, respectively. According to Kubo' s Stochastic Line Shape Theory,[61] the dipole moment is assumed as

$$\frac{d\mu}{dt} = i\omega(t)\mu \quad (9)$$

$$\omega(t) = \bar{\omega} + \delta\omega(t) \quad (10)$$

then, in Condon approximation, we change the (8) into[62]

$$I^{con}(\omega) \sim |\langle \mu_{10} \rangle|^2 \int_0^\infty dt e^{-i\omega t + i\bar{\omega}_{10} t} \langle e^{i\int_0^t d\tau \delta\omega_{10}(\tau)} \rangle e^{-t/2T_1} \quad (11)$$

Here, $\bar{\omega}_{10}$ is the average of the transition frequency from υ =1 to υ =0 and $\delta\omega$ is the fluctuation amplitude of the transition frequency at τ . $\langle \mu_{10} \rangle$ is the average of the transition dipole moment between vibrational states 1 and 0. $e^{-t/2T_1}$ describes the damping property of the line shape. T_1 is the life time of the υ =1 state which can affect the line shape of the 1D spectrum. We obtain the lifetime T_1 through fitting the width at half maximum of the theoretical peak with the experimental value and it will be brought into the three order response function to explore the dephasing process between the 1-0 resonance and 2-1 resonance. The equation of the cumulant expansion truncated at second order is given as[62]

$$I^{cum}(\omega) \sim |\mu_{10}|^2 \int_0^\infty dt e^{-i\omega t + i\omega_{10} t} e^{-g_{10,10}(t)} e^{-t/2T_1} \quad (12)$$

$$g_{10,10}(t) = \int_0^\infty d\tau (t-\tau) \langle \delta\omega_{10}(t) \cdot \delta\omega_{10}(0) \rangle \quad (13)$$

Where is denoted as the line shape of the cumulant expansion spectrum.

2.3. Calculation of 2-dimensional (2D) spectra. The 2D pump-probe spectroscopy is the three order response function after phase matching. The external fields are interacted with the three levels system which we mentioned above (ψ_0, ψ_1, ψ_2) in two phase-matched ways: the rephrasing way and the non-rephasing way,[63] with the directions of wave vectors $\vec{k_{\mathrm{I}}} = -\vec{k_1} + \vec{k_2} + \vec{k_3}$ and $\vec{k_{\mathrm{II}}} = \vec{k_1} - \vec{k_2} + \vec{k_3}$ respectively, where $\vec{k_1}$, $\vec{k_2}$ and $\vec{k_3}$ are the wave vector of the incoming fields. The phase matching process is illustrated by double sides Feynman diagrams in figure 3. The time t_1 represents the time between the first two pulses, while the time t_2 represents the time between the second two pulses. And the results of the signal are detected at time t_3 after the third pulse. The response functions of rephrasing R_{re} and non-rephasing R_{non} with the cumulant expansion truncated at second order are given as[64,65]

$$\begin{aligned} R_{\mathrm{re}} = 2|\mu_{10}|^4 \exp[&i\bar{\omega}_{10}(t_1 - t_3) - g_{10,10}(t_1) + g_{10,10}(t_2) \\ &- g_{10,10}(t_3) - g_{10,10}(t_1 + t_2) - g_{10,10}(t_2 + t_3) + g_{10,10} \\ &(t_1 + t_2 + t_3)] \exp(-\frac{t_3}{2T_1} - \frac{t_2}{T_1} - \frac{t_1}{2T_1}) - |\mu_{10}|^2 |\mu_{21}|^2 \\ &\exp[i\bar{\omega}_{10} t_1 - i\bar{\omega}_{21} t_3 - g_{10,10}(t_1) + g_{10,21}(t_2) - g_{21,21} \\ &(t_3) - g_{10,21}(t_1 + t_2) - g_{10,21}(t_2 + t_3) + g_{10,21}(t_1 + t_2 \\ &+ t_3)] \exp[-(\frac{1}{2T_2} + \frac{1}{2T_1}) t_3 - \frac{t_2}{T_1} - \frac{t_1}{2T_1}] \end{aligned} \quad (13)$$

$$\begin{aligned} R_{\mathrm{non}} = 2|\mu_{10}|^4 \exp[&-i\bar{\omega}_{10}(t_1 + t_3) - g_{10,10}(t_1) - g_{10,10}(t_2) \\ &- g_{10,10}(t_3) + g_{10,10}(t_1 + t_2) + g_{10,10}(t_2 + t_3) - g_{10,10} \\ &(t_1 + t_2 + t_3)] \exp(-\frac{t_3}{2T_1} - \frac{t_2}{T_1} - \frac{t_1}{2T_1}) - |\mu_{10}|^2 |\mu_{21}|^2 \\ &\exp[-i\bar{\omega}_{10} t_1 - i\bar{\omega}_{21} t_3 - g_{10,10}(t_1) - g_{10,21}(t_2) - g_{21,21} \\ &(t_3) + g_{10,21}(t_1 + t_2) + g_{10,21}(t_2 + t_3) - g_{10,21}(t_1 + t_2 \\ &+ t_3)] \exp[-(\frac{1}{2T_2} + \frac{1}{2T_1}) t_3 - \frac{t_2}{T_1} - \frac{t_1}{2T_1}] \end{aligned} \quad (14)$$

Where we assume that the lifetime T_2 is equated to $T_1/2$[65] and the signals are converted to the frequency domain using two-dimension Fourier transforms of the time t_1 and t_3

$$S_{\mathrm{re}}^{(3)}(\omega_1,t_2,\omega_3)=\int_0^\infty\int_0^\infty R_{re}\cdot\exp[i(\omega_3 t_3-\omega_1 t_1)]\,dt_3dt_1 \quad (15)$$

$$S_{\mathrm{non}}^{(3)}(\omega_1,t_2,\omega_3)=\int_0^\infty\int_0^\infty R_{non}\cdot\exp[i(\omega_3 t_3+\omega_1 t_1)]\,dt_3dt_1 \quad (16)$$

Finally, the 2D pump-probe spectrum is obtained as the imaginary part of the sum of both rephrasing signal and non-rephasing signal. The results will be discussed in the section of RESULTS AND DISCUSS.

2.4. Ab Initio Molecular Dynamics Simulations Setup. Ab Initio Molecular Dynamics simulations within the framework of classical nuclei motion were performed with the CPMD simulation package (see http://www.cpmd.org/). The BLYP functional[66,67] in conjunction with added dispersion corrections[68] was used together with norm-conserving pseudo-potentials[69] for core electrons and the plane wave basis set with cutoff energy of 70 Ry for active valance electrons. The energies, dipole moments and the forces were calculated as the system is propagated in classical dynamics way on the local Born-Oppenheimer surface and the Born-Oppenheimer Molecular Dynamics (BOMD)[70] is employed in the simulation with a time step of 30 au ≈ 0.72fs. For all simulations of the systems $(HCl)_m(H_2O)_n$ (m=1,2; n=1,2,3), the massive Nosé-Hoover thermostats[71] were applied to generate a trajectory (which is recorded at step time of 90 au, and the dipole moments is recorded at the same time) in the canonical ensemble (NVT) which kept the temperature of the nucleus at 200k. The Poisson equation is solved by using the Martyna-Tuckerman solver[72] for molecules in a box of 15Å side length. During all simulations the total linear and angular momentum were corrected to zero at every 100 steps.

3. RESULTS AND DISCUSS

3.1.1. The HCl stretching vibrational mode in $HCl(H_2O)_1$. The spectra of the HCl stretching vibration in $HCl(H_2O)_1$ is shown in Figure 4. The 1D IR results of the HCl stretching vibrational frequency of the $HCl(H_2O)_1$ cluster (the red solid line in figure 4(c)) is located at 2710.75 cm^{-1} with CCSD(T)-F12b-based potential, only 12.8 cm^{-1} away from the experimental value,[16,17] 2723.5 cm^{-1}. Compared with the peak which is obtained from the Fourier transform of DAF is 203.5 cm^{-1} away from the experimental value, the new method has a remarkable improvement of this DAF method (the red solid line in figure 4(a) represents the DAF method with the functional BLYP-based potential) which is modified by high-temperature (or harmonic) quantum correction factor.[73] In addition, the 12.78 cm^{-1} deviation from the experimental value may come from the error of the potential CCSD(T)-F12b/cc-pVTZ-F12 and the neglect of the quantum effect of other DOFs. The spectrum obtained by the Fourier transform of the distance autocorrelation function (DISAF) is given as

$$I(\omega)\sim\int_0^\infty dt e^{-i\omega t}\langle \boldsymbol{d}(0)\cdot\boldsymbol{d}(t)\rangle \quad (17)$$

Figure 4(a) is illustrated that the vibrational frequency obtained by the DAF method is consistent with the DISAF method which is also modified by high-temperature (or harmonic) quantum correction factor. It indicates that the dipole moment which is calculated during BOMD simulation reflects that the nucleus move classically, but the line shape of DAF is better than DISAF compared with the experimental results. The main shortcoming of the DAF method is the failure to include the quantum effect of the stretching vibrational motion of the nucleus.[26] Compared between the red solid line and the green dashed line in (c), there is not much difference of the results between Condon

approximation and cumulant expansion in $HCl(H_2O)_1$ cluster, which indicates that the environment (a H_2O molecule) affects the frequency fluctuation of the HCl stretching vibration in Gaussian-like distribution. Table 1 indicates the peak of the DAF method (the dipole moment is calculated with BLYP-based potential) centered at 2520 cm^{-1}, while the peak which is calculated with BLYP-based potential in the new method centered at $2628.08\ cm^{-1}$, $95.42\ cm^{-1}$ away from the experimental peak. The different between those two results is 108.08 cm^{-1} which can be regarded as the contribution of the quantum effect of the HCl stretching vibration at the same calculated level. The difference between the functionals, the M06-2x and BLYP, is 61.57 cm^{-1}, and the vibrational frequency of the functional M06-2x is closer to the experimental value. In the table 1, the vibrational analysis[17,26,74] (VA) results which include the harmonics frequencies with the HF and post-HF (MP2 and CCSD(T)-F12b methods) levels have overestimated the vibrational frequency comparing with the experimental measure. Apart from the failure to include the part of anharmonic frequency, VA can only obtain the frequency at the corresponding energy minima which lead to the failure to calculate the vibrational frequencies of the special vibrational mode with the time evolution. The VA is also limited with the size of a molecule or a cluster because the harmonic frequency of a specific vibrational mode is obtained after the calculation of the second-order partial derivatives of the potential, which is computationally expansive.

3.1.2. The 2D pump-probe spectra between the 1-0 resonance and 2-1 resonance of the HCl stretching vibrational mode in the $HCl(H_2O)_1$ cluster. The 2D pump-probe spectra are carried out with the time t_2 evolution. They represent the HCl stretching vibration of the $HCl(H_2O)_1$ cluster with the CCSD(T)-F12b-based potential. The ω_1 axis represents the measure of the pump pulse and the ω_3 axis represents the measure of the probe pulse. The projection on the ω_3 axis is the dynamical line shape both the 1-0 resonance (warm colors) and the 2-1 resonance (cold colors). The anharmonicity of the vibrational mode is obtained as $160 \pm 5 cm^{-1}$ when the evolution time t_2 is close to the lifetime of the two resonances coupling. As the time t_2 is increasing, the dynamical line shape is broadened and the nodal slope is reducing. The nodal slope (figure 6) is approached to zero, when the time t_2 is close to nearly 1.1 ps. Thus, we are regarded the 1.1 ps as the period of the dephasing process approximately, which can be used as the assessment of the dephasing experiment of the vibrational modes or some theoretical investigation behind the results.

3.2. The HCl stretching vibration of C-H--O in $(HCl)_2(H_2O)_1$. The line shape of the main peak in Figure 7 which is centered at 2565.3 cm^{-1} is in good agreement with the experimental peak and has only 14.7 cm^{-1} red shift from the experimental vibrational frequency. The three small peaks, left side of the main peak, are derived from the unstable structure of the $(HCl)_2(H_2O)_1$ cluster. The theoretical spectrum of figure 7 indicates that the small peaks may contribute to the band of the small peaks spun from S_8 to S_{10} in experimental spectrum.

3.3. The HCl stretch in $HCl(H_2O)_2$. The spectroscopic information of the HCl stretching vibrational mode of the 1:2 cluster illustrated in Figure 7 is at 2407 cm^{-1} which is left side of the experimental peak located at 2460 cm^{-1}. The line shape is a little narrower than the experimental line shape S_{10}. The small peaks next to the S_{10} (theoretical spectrum in figure 7) may be derived from some microscopic structure of the $HCl(H_2O)_2$ cluster whose frequencies are blue shift appear frequently during the MD simulation.

3.4. The HCl stretch in $HCl(H_2O)_3$ and the dissociated threshold of the HCl. In the Figure 7, we give a predicted HCl stretching vibrational character band of the 1:3 cluster centered at 2246.5 cm^{-1} and there is no correlated experiment assignment due to the $HCl(H_2O)_3$ cluster is very close to the dissociated threshold and the concentration of the cluster is very low in the mix measured expansions.[16,17] In figure 8(c), the distance between the acidic proton and Cl atom (red line in figure 8(c)) is close to the distance between the H atom of the adjacent H_2O and the O atom of the adjacent H_2O (green line and laurel-green line in figure 8(c)). But the H-Cl bond distance has changed little compared with the H-Cl bond distances of the $HCl(H_2O)_1$, $HCl(H_2O)_2$ clusters. The adjacent O approached the H atom of the HCl molecule gradually with the n of $HCl(H_2O)_n$ increasing from n=1 to n=3. When n increased to the qualitative change point, n=4, the blue line overlapped with the green, laurel-green line under the red line at the simulation time between 1ps and 3.5ps (figure 8(d)), which means the H_3O^+ ion and the Cl^- ion have formed. The recent experiment of the HCl-water clusters in helium droplets has confirmed that the spectrally broad background signal at 2675 cm^{-1} is contributed by the HCl stretching vibration of the dissociated $HCl(H_2O)_4$ cluster.[24] At the simulation time of the range from 4ps to 10ps, the H^+ ion leave the adjacent O and the acidic proton stayed in the middle of the Cl and O atom at the simulation time after 10ps. The simulations are illustrated that the structure of $HCl(H_2O)_3$ is on the margin of the dissociated structure and the dissociated structure as a stable state exits on a minimum point of the free energy surface of the $HCl(H_2O)_4$ cluster at 200k.

4. CONCLUSIONS

The precise description of the IR spectroscopy of a certain chromophore needs the precise enough potential models which can lead a reasonable microscopic dynamical simulation and the recording of the precise transition dipoles or frequencies with the time evolution. As the size of such hydrogen-bonded systems increases, the IR spectroscopic lines become congested and display highly complex line shapes due to the strong interaction,[49] which are difficult to make assignments and analyze the microscopic dynamics in both theories and experiments. Thus, it has a fundamental significance to abstract a specific vibrational mode and describe the spectroscopic line of this vibrational mode precisely. A new spectra calculated method which has a remaekable improvement of the DAF method has been proposed. The method can cover all the contribution of the quantum effect of the HCl stretching vibration because the vibrational wave function can be accurately described by solving the 1D Schrödinger equation. Other DOFs can be regarded as classical motion safely. We can abstract any specific vibrational mode, or investigate any coupling of two vibrational modes through the method. In theoretical speaking, we can descript the accurate spectra if the force flied is good enough.

However, there are still some deficiencies in present calculation. For the case of the dissociated $HCl(H_2O)_4$ cluster, the degenerate states exist during the dissociated process and the multistate force field should be employed. Ab initio force fields are limited by the size of the studied system and are impossible to apply them into the biology system. The path integral molecular dynamics or the quantum wave packet dynamics can be used to observe the behavior of the quantum effect, which will be reported by our future work.

AUTHOR INFORMATION

Corresponding Author

Prof_huili@jlu.edu.cn

jiali@jialigao.org

Notes

The authors declare no competing financial interest.

ACKNOWLEDGMENT

Authors thank Prof. Dr. Martin A. Suhm and Dr. Michal Fárník to supply the raw experimental data. This research has been supported by the National Natural Science Foundation of China (Grant Nos. 21003058 and 21273094), Program for New Century Excellent Talents in University and the National Institutes of Health (Grant No. GM46376).

REFERENCES

(1) Packer, M. J.; Clary, D. C. *J. Phys. Chem.* **1995**, *99*, 14323.

(2) Rowland, S. F. *Annu. Rev. Phys. Chem.* **1991**, *42*, 731.

(3) Abbatt, J. P. D.; Molina, M. J. *J. Phys. Chem.* **1992**, *96*, 7674.

(4) Gertner, B. J.; Hynes, J. T. *Science* **1996**, *271*, 1563.

(5) McNeill, V. F.; Loerting, T.; Geiger, F. M.; Trout, B. L.; Molina, M. J. *PNAS* **2006**, *103*, 9422.

(6) Huthwelker, T.; Ammann, M.; Peter, T. *Chem. Rev.* **2006**, *106*, 1375.

(7) Talukdar, R. K.; Burkholder, J. B.; Roberts, J. M.; Portmann, R. W.; Ravishankara, A. R. *J. Phys. Chem. A* **2012**, *116*, 6003.

(8) Walewski, Ł.; Forbert, H.; Marx, D. *ChemPhysChem* **2013**, *14*, 817.

(9) Walewski, Ł.; Forbert, H.; Marx, D. *J. Phys. Chem. Lett.* **2011**, *2*, 3069.

(10) Sugawara, S.; Yoshikawa, T.; Takayanagi, T.; Tachikawa, M. *Chem. Phys. Lett.* **2011**, *501*, 238.

(11) Takayanagi, T.; Takahashi, K.; Kakizaki, A.; Shiga, M.; Tachikawa, M. *Chem. Phys.* **2009**, *358*, 196.

(12) Gutberlet, A.; Schwaab, G.; Birer, Ö.; Masia, M.; Kaczmarek, A.; Forbert, H.; Havenith, M.; Marx, D. *Science* **2009**, *324*, 1545.

(13) Odde, S.; Mhin, B. J.; Lee, S.; Lee, H. M.; Kim, K. S. *J. Chem. Phys.* **2004**, *120*, 9524.

(14) Forbert, H.; Masia, M.; Kaczmarek-Kedziera, A.; Nair, N. N.; Marx, D. *J. Am. Chem. Soc.* **2011**, *133*, 4062.

(15) Leopold, K. R. *Annu. Rev. Phys. Chem.* **2011**, *62*, 327.

(16) Weimann, M.; Farnik, M.; Suhm, M. A. *Phys. Chem. Chem. Phys.* **2002**, *4*, 3933.

(17) Fárník, M.; Weimann, M.; Suhm, M. A. *J. Chem. Phys.* **2003**, *118*, 10120.

(18) Huneycutt, A. J.; Stickland, R. J.; Hellberg, F.; Saykally, R. J. *J. Chem. Phys.* **2003**, *118*, 1221.

(19) Ortlieb, M.; Birer, Ö.; Letzner, M.; Schwaab, G. W.; Havenith, M. *J. Phys. Chem. A* **2007**, *111*, 12192.

(20) Skvortsov, D.; Lee, S. J.; Choi, M. Y.; Vilesov, A. F. *J. Phys. Chem. A* **2009**, *113*, 7360.

(21) Zwier, T. S. *Science* **2009**, *324*, 1522.

(22) Flynn, S. D.; Skvortsov, D.; Morrison, A. M.; Liang, T.; Choi, M. Y.; Douberly, G. E.; Vilesov, A. F. *J. Phys. Chem. Lett.* **2010**, *1*, 2233.

(23) Morrison, A. M.; Flynn, S. D.; Liang, T.; Douberly, G. E. *J. Phys. Chem. A* **2010**, *114*, 8090.

(24) Letzner, M.; Gruen, S.; Habig, D.; Hanke, K.; Endres, T.; Nieto, P.; Schwaab, G.; Walewski, Ł.; Wollenhaupt, M.; Forbert, H.; Marx, D.; Havenith, M. *J. Chem. Phys.* **2013**, *139*.

(25) la Cour Jansen, T.; Knoester, J. *J. Chem. Phys.* **2006**, *124*.

(26) Masia, M.; Forbert, H.; Marx, D. *J. Phys. Chem. A* **2007**, *111*, 12181.

(27) Lin, W.; Paesani, F. *J. Phys. Chem. A* **2013**, *117*, 7131.

(28) Hassanali, A. A.; Cuny, J.; Ceriotti, M.; Pickard, C. J.; Parrinello, M. *J. Am. Chem. Soc.* **2012**, *134*, 8557.

(29) Lee, C.; Sosa, C.; Planas, M.; Novoa, J. J. *J. Chem. Phys.* **1996**, *104*, 7081.

(30) Bacelo, D. E.; Binning, R. C.; Ishikawa, Y. *J. Phys. Chem. A* **1999**, *103*, 4631.

(31) Milet, A.; Struniewicz, C.; Moszynski, R.; Wormer, P. E. S. *J. Chem. Phys.* **2001**, *115*, 349.

(32) Estrin, D. o. A.; Kohanoff, J.; Laria, D. H.; Weht, R. O. *Chem. Phys. Lett.* **1997**, *280*, 280.

(33) Chaban, G. M.; Gerber, R. B.; Janda, K. C. *J. Phys. Chem. A* **2001**, *105*, 8323.

(34) Daniel Boese, A.; Forbert, H.; Masia, M.; Tekin, A.; Marx, D.; Jansen, G. *Phys. Chem. Chem. Phys.* **2011**, *13*, 14550.
(35) Sillanpää, A.; Laasonen, K. *ChemPhysChem* **2005**, *6*, 1879.
(36) Ndongmouo, U. F. T.; Lee, M. S.; Rousseau, R.; Baletto, F.; Scandolo, S. *J. Phys. Chem. A* **2007**, *111*, 12810.
(37) Re, S.; Osamura, Y.; Suzuki, Y.; Schaefer, H. F. *J. Chem. Phys.* **1998**, *109*, 973.
(38) Devlin, J. P.; Uras, N.; Sadlej, J.; Buch, V. *Nature* **2002**, *417*, 269.
(39) Planas, M.; Lee, C.; Novoa, J. J. *J. Phys. Chem.* **1996**, *100*, 16495.
(40) Mancini, J. S.; Bowman, J. M. *J. Chem. Phys.* **2013**, *138*.
(41) Mancini, J. S.; Samanta, A. K.; Bowman, J. M.; Reisler, H. *J. Phys. Chem. A* **2014**, *118*, 8402.
(42) Mancini, J. S.; Bowman, J. M. *J. Phys. Chem. A* **2014**, *118*, 7367.
(43) Mancini, J. S.; Bowman, J. M. *J. Phys. Chem. Lett.* **2014**, *5*, 2247.
(44) Samanta, A. K.; Czakó, G.; Wang, Y.; Mancini, J. S.; Bowman, J. M.; Reisler, H. *Acc. Chem. Res.* **2014**, *47*, 2700.
(45) Knizia, G.; Adler, T. B.; Werner, H.-J. *J. Chem. Phys.* **2009**, *130*.
(46) Zhao, Y.; Truhlar, D. *Theor. Chem. Acc.* **2008**, *120*, 215.
(47) Paesani, F.; Xantheas, S. S.; Voth, G. A. *J. Phys. Chem. B* **2009**, *113*, 13118.
(48) Bakker, H. J.; Skinner, J. L. *Chem. Rev.* **2009**, *110*, 1498.
(49) Nibbering, E. T. J.; Elsaesser, T. *Chem. Rev.* **2004**, *104*, 1887.
(50) Li, H.; Blinov, N.; Roy, P.-N.; Le Roy, R. J. *J. Chem. Phys.* **2009**, *130*, 144305.
(51) Li, H.; Ma, Y.-T. *J. Chem. Phys.* **2012**, *137*.
(52) Colbert, D. T.; Miller, W. H. *J. Chem. Phys.* **1992**, *96*, 1982.
(53) Light, J. C.; Hamilton, I. P.; Lill, J. V. *J. Chem. Phys.* **1985**, *82*, 1400.
(54) Coxon, J. A.; Hajigeorgiou, P. G. *J. Mol. Spectrosc.* **2000**, *203*, 49.
(55) Kubo, R. In *Adv. Chem. Phys.*; John Wiley & Sons, Inc.: 2007, p 101.
(56) Skinner, J. L. *Mol. Phys.* **2008**, *106*, 2245.
(57) Cho, M. *Chem. Rev.* **2008**, *108*, 1331.
(58) Mukamel, S. *Principles of Nonlinear Optical Spectroscopy*, Oxford: London, 1995.
(59) Kwac, K.; Lee, H.; Cho, M. *J. Chem. Phys.* **2004**, *120*, 1477.
(60) Becke, A. D. *Phys. Rev. A* **1988**, *38*, 3098.
(61) Lee, C.; Yang, W.; Parr, R. G. *Phys. Rev. B* **1988**, *37*, 785.
(62) Grimme, S. *J. Comput. Chem.* **2006**, *27*, 1787.
(63) Troullier, N.; Martins, J. L. *Phys. Rev. B* **1991**, *43*, 1993.
(64) Barnett, R. N.; Landman, U. *Phys. Rev. B* **1993**, *48*, 2081.
(65) Martyna, G. J.; Klein, M. L.; Tuckerman, M. *J. Chem. Phys.* **1992**, *97*, 2635.
(66) Martyna, G. J.; Tuckerman, M. E. *J. Chem. Phys.* **1999**, *110*, 2810.
(67) Ramírez, R.; López-Ciudad, T.; Kumar P, P.; Marx, D. *J. Chem. Phys.* **2004**, *121*, 3973.
(68) Garcia-Viloca, M.; Nam, K.; Alhambra, C.; Gao, J. *The Journal of Physical Chemistry B* **2004**, *108*, 13501.

Table 1. The HCl stretching vibrational frequency $\upsilon_{\text{Cl-H}}/\text{cm}^{-1}$ and the blue shift $\Delta\upsilon_{\text{Cl-H}}/\text{cm}^{-1}$ with respect to experimental values of the $HCl(H_2O)_1$ cluster are compared among VA, DD and TW. The data in VA part are obtained from reference 1

and 2[a].

	Method	Basis Set	$\upsilon_{\text{Cl-H}}$	$\Delta\upsilon_{\text{Cl-H}}$ [b]
	HF	Q[c]	3033.0	309.5
VA[16,17]	MP2	T[c]	2791.0	67.5
	CCSD(T)	D[c]	2782.0	58.5
DAF	BLYP	PW[d]	2520	-203.5
	BLYP	PW[d]	2628.1	-95.4
TW	M06-2x	cc-pVTZ	2689.6	-33.9
	CCSD(T)-F12	cc-pVTZ-F12	2710.7	-12.8
EXP[16,17]			2723.5	

[a]Abbreviations is used as: VA=Vibrational Analysis, DD= Dipole Autocorrelation Function, PW=Plane Wave, TW=This Work. [b] $\Delta\upsilon_{\text{Cl-H}} = \upsilon_{\text{Cl-H}} - \upsilon_{\text{Exp}}$ [c]aug-cc-pVXZ, X=D,T,Q. [d]The plane wave is generated by the 15Å side length box and the 70 Ry cutoff energy.

Figure 1. The vibrational wave functions of the ground, first excited and second excited states of an isolated HCl molecule.

Figure 2. The HCl stretching vibrational frequency shift of the HCl-water cluster is compared with the free HCl molecule.

Figure 3. The double-sided Feynman diagrams represent eight Liouville space pathways in three levels system. The R_1, R_2, and R_3 are denoted as a rephrasing process, while the R_3, R_4, and R_6 are denoted as a non-rephasing process. R_7, R_8 are neglected in response function because they are not accorded with either of two phase matching directions.

Figure 4. Comparison between the experimental and theoretical spectra of the HCl stretching vibration of the $HCl(H_2O)_1$ cluster. (a) Comparison between the experimental result (blue solid) and the spectrum transformed from DAF (red solid) obtained by equ. (8) and from DISAF (olive green dashed) obtained by equ. (17). The new method with the BLYP-based (red solid) and M06-2x-based (pink dashed) potential are expressed in (b). The red solid line in (c) represents the spectroscopic line of our new method based on CCSD(T)-F12 potential in Condon approximation and the olive green dashed line is calculated based on the cumulant expansion truncated at second order. The pink dashed line, in the (c), represents the distribution of the CCSD(T)-F12-based frequency.

Figure 5. The 2D pump-probe spectra of the HCl stretching vibration of the $HCl(H_2O)_1$ cluster at the evolution time t_2 = 0 fs, 360 fs, 840 fs and 1008 fs.

Figure 6. The nodal slope of the straight lines which separate the 1-0 resonance (warm colors) and the 2-1 resonance (cold colors) in 2D pump-probe spectra.

Figure 7. The sum of the HCl stretching vibrational spectra of the $(HCl)_1(H_2O)_1$, $(HCl)_2(H_2O)_1$, $(HCl)_1(H_2O)_2$ and $(HCl)_1(H_2O)_3$ clusters with the weight factors for the relative intensities 1, 0.29, 0.26 and 0.1, and compared it with the experimental spectra. The S_3, S_8 and S_{10} are donated as HCl stretching vibration of the $(HCl)_1(H_2O)_1$, $(HCl)_2(H_2O)_1$, $(HCl)_1(H_2O)_2$, respectively.

Figure 8. The distances between the acidic proton and Cl atom (red line), the acidic proton and the O atom of the adjacent H_2O (blue dashed line), two H atoms of the adjacent H_2O and the O atom of the adjacent H_2O (green line and pink line).

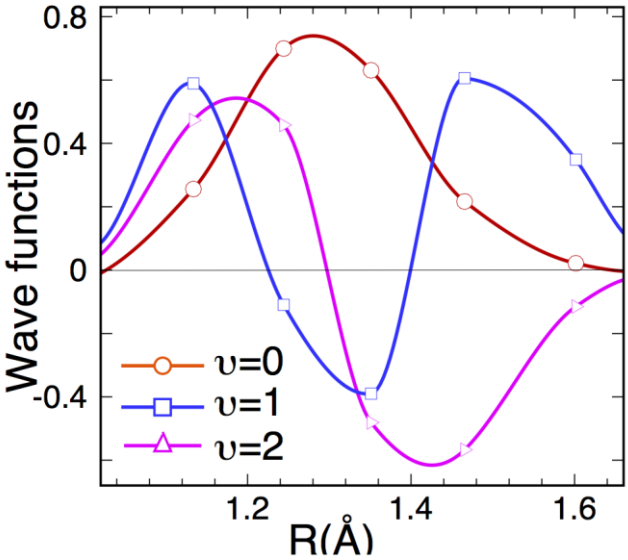

Figure 1

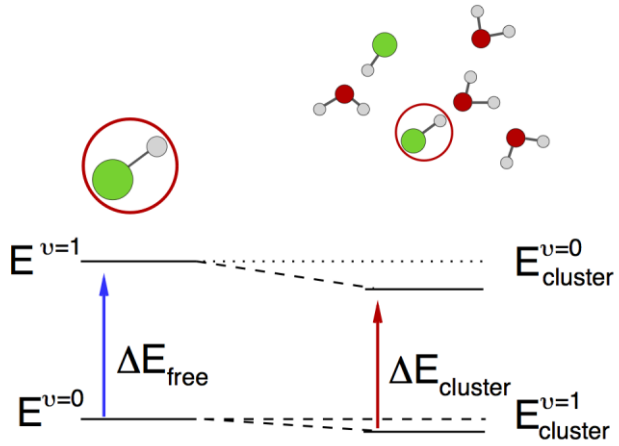

Figure 2

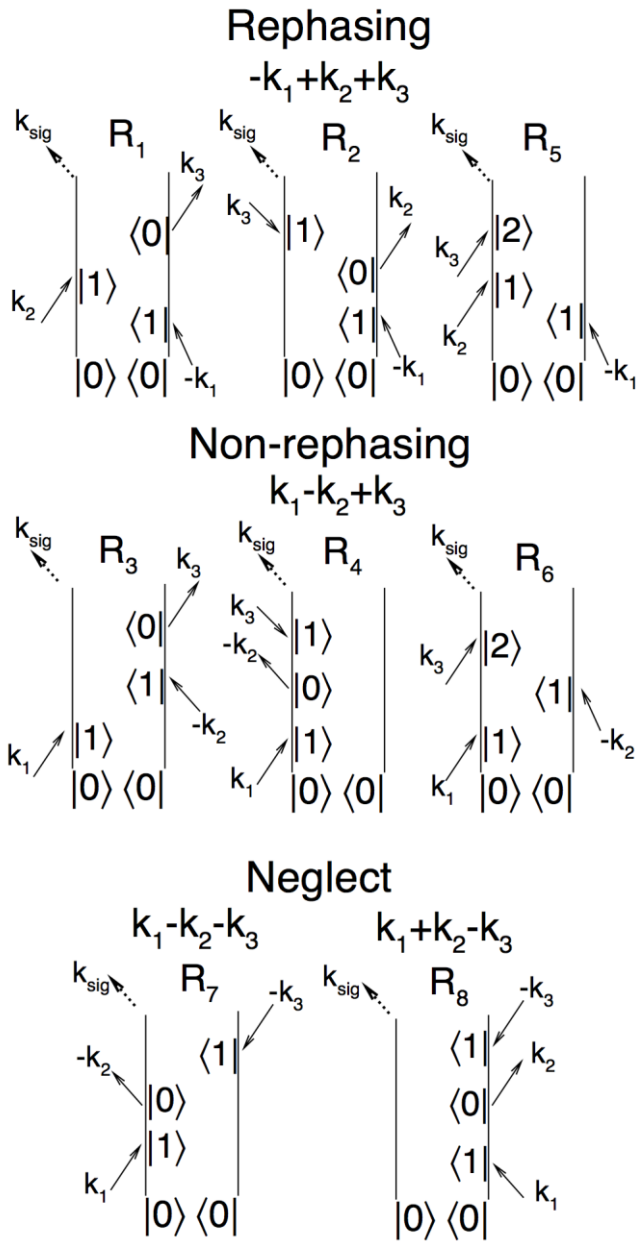
Rephasing
-k1+k2+k3
ksig
R1
k3
⟨0|
k2
|1⟩
⟨1|
|0⟩ ⟨0|
-k1
ksig
R2
k3
|1⟩
k2
⟨0|
⟨1|
|0⟩ ⟨0|
-k1
ksig
R5
|2⟩
k3
|1⟩
k2
⟨1|
|0⟩ ⟨0|
-k1
Non-rephasing
k1-k2+k3
ksig
R3
k3
⟨0|
⟨1|
-k2
k1
|1⟩
|0⟩ ⟨0|
ksig
R4
k3
|1⟩
-k2
|0⟩
k1
|1⟩
|0⟩ ⟨0|
ksig
R6
|2⟩
k3
⟨1|
-k2
|1⟩
k1
|0⟩ ⟨0|
Neglect
k1-k2-k3
ksig
R7
-k3
⟨1|
-k2
|0⟩
|1⟩
k1
|0⟩ ⟨0|
k1+k2-k3
ksig
R8
-k3
⟨1|
k2
⟨0|
⟨1|
k1
|0⟩ ⟨0|

Figure 3

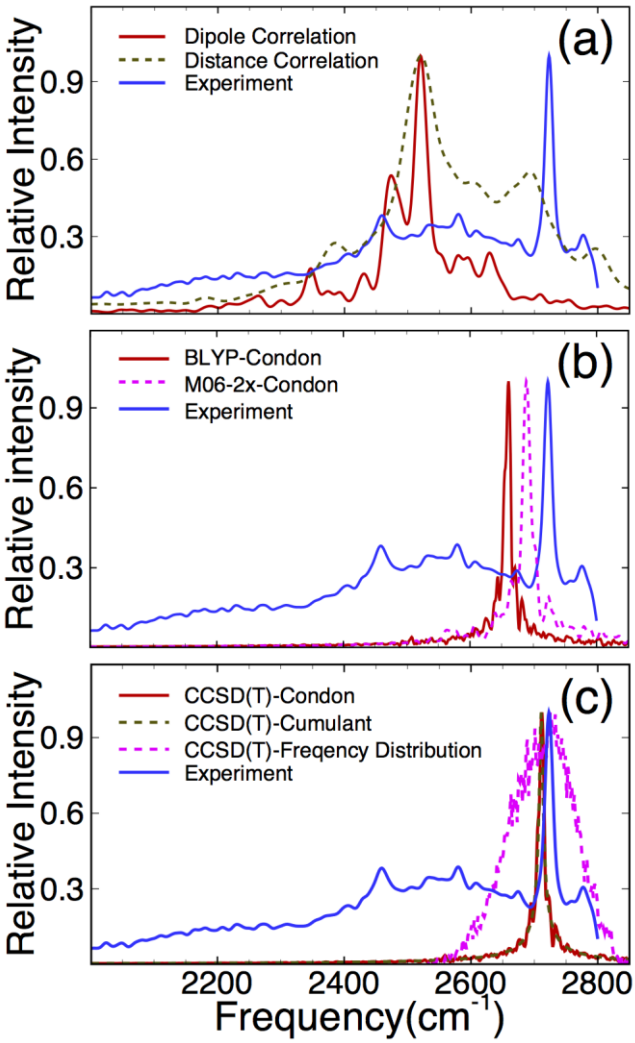
(a)
Dipole Correlation
Distance Correlation
Experiment
Relative Intensity
0.9
0.6
0.3
(b)
BLYP-Condon
M06-2x-Condon
Experiment
Relative intensity
0.9
0.6
0.3
(c)
CCSD(T)-Condon
CCSD(T)-Cumulant
CCSD(T)-Freqency Distribution
Experiment
Relative Intensity
0.9
0.6
0.3
2200
2400
2600
2800
Frequency(cm-1)

Figure 4

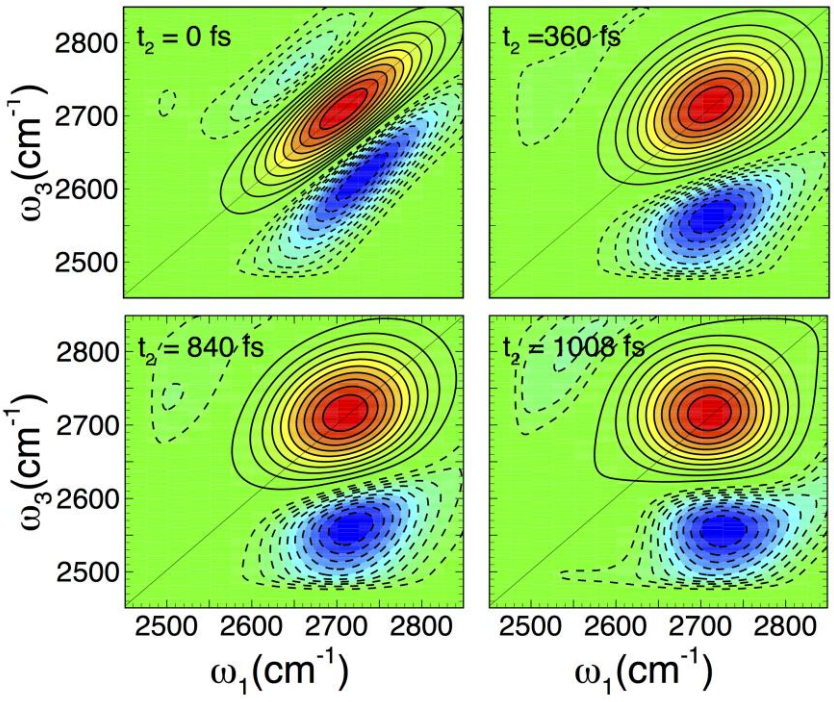
t2 = 0 fs
t2 =360 fs
t2 = 840 fs
t2 = 1008 fs
ω3(cm-1)
ω1(cm-1)
2500
2600
2700
2800

Figure 5

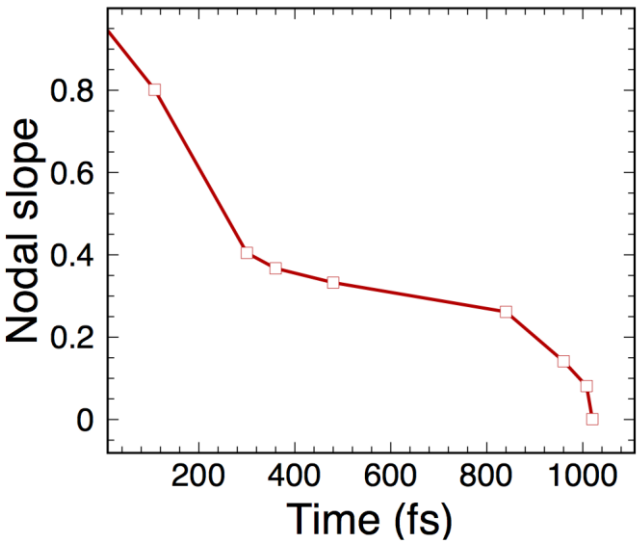

Figure 6

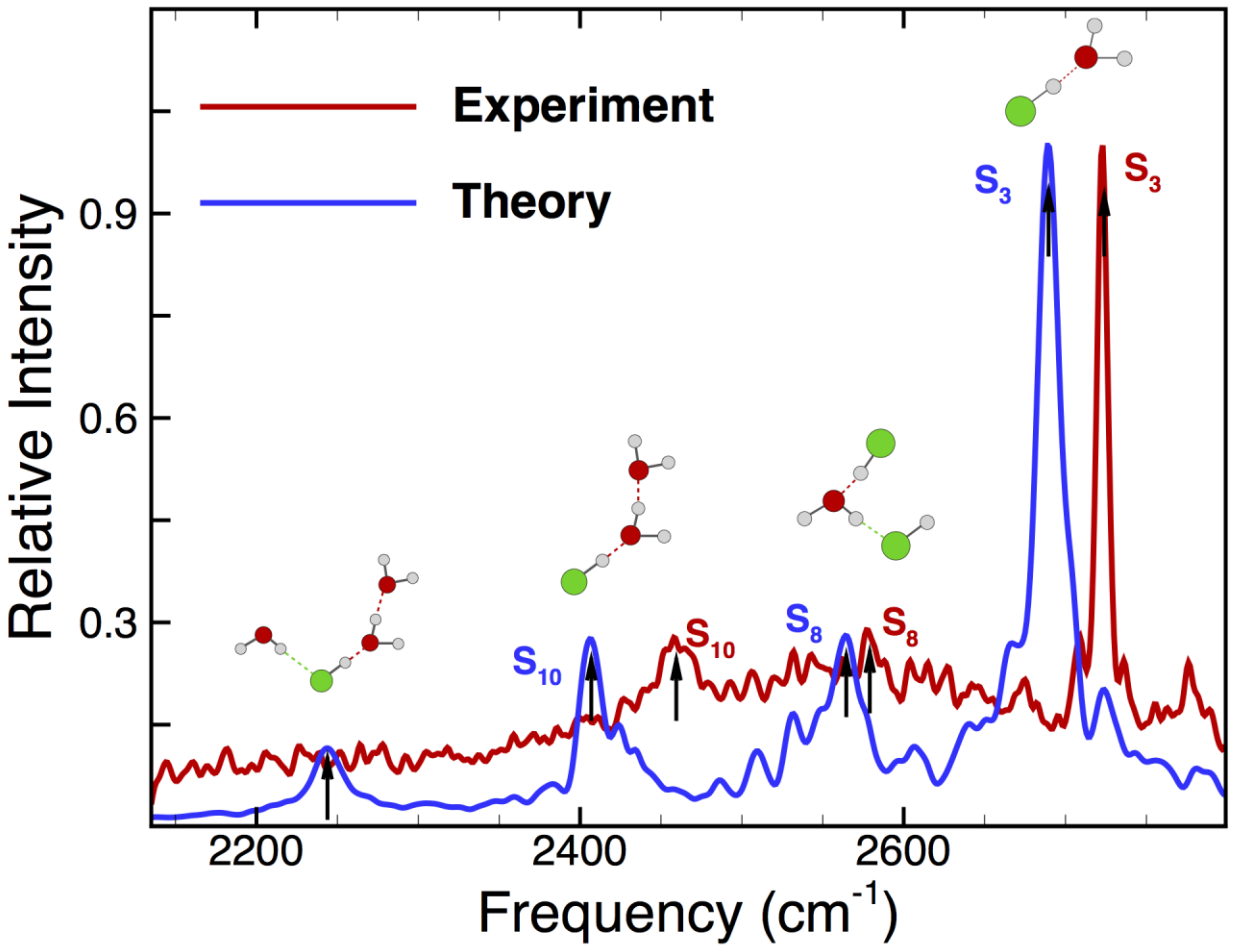
Experiment
Theory
Relative Intensity
0.9
0.6
0.3
2200
2400
2600
Frequency (cm-1)
S3
S3
S10
S10
S8
S8

Figure 7

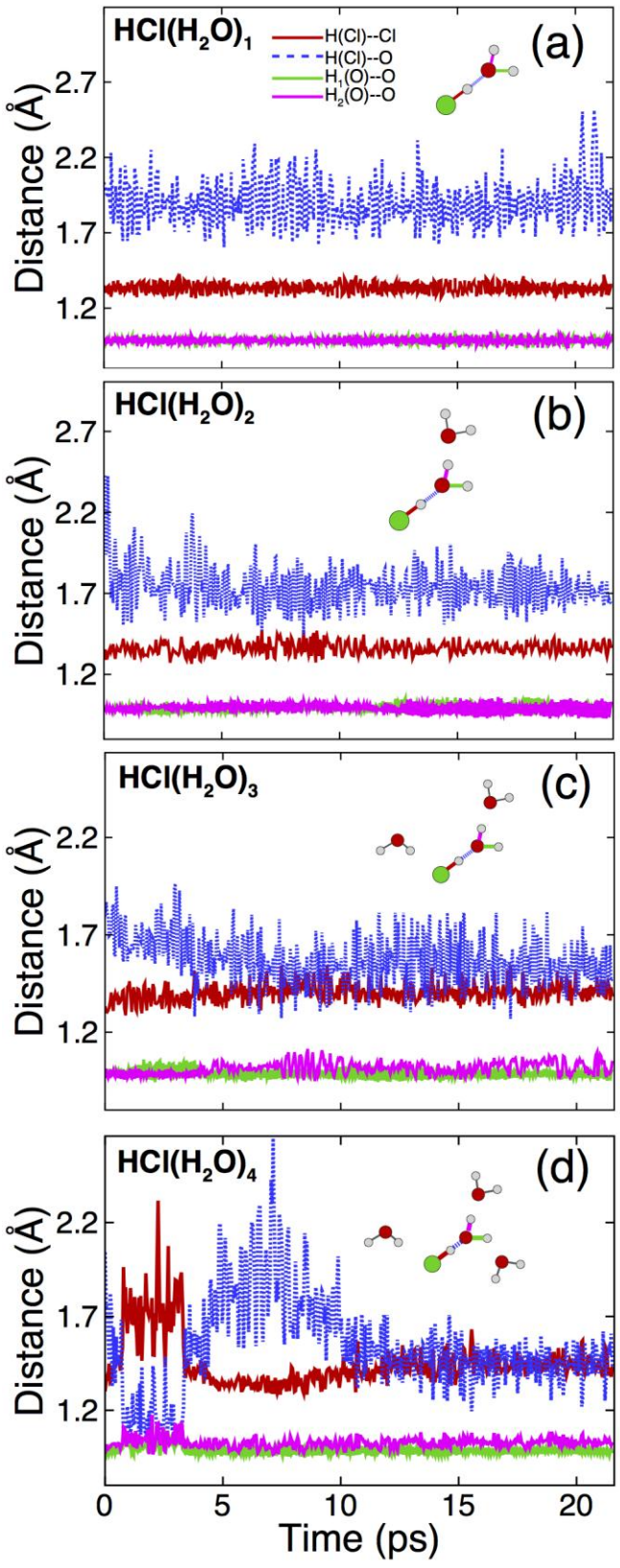
HCl(H2O)1
H(Cl)--Cl
H(Cl)--O
H1(O)--O
H2(O)--O
(a)
HCl(H2O)2
(b)
HCl(H2O)3
(c)
HCl(H2O)4
(d)
Distance (Å)
2.7
2.2
1.7
1.2
0
5
10
15
20
Time (ps)

Figure 8

(1) Packer, M. J.; Clary, D. C. *J. Phys. Chem.* **1995**, *99*, 14323.
(2) Rowland, S. F. *Annu. Rev. Phys. Chem.* **1991**, *42*, 731.
(3) Abbatt, J. P. D.; Molina, M. J. *J. Phys. Chem.* **1992**, *96*, 7674.
(4) Gertner, B. J.; Hynes, J. T. *Science* **1996**, *271*, 1563.
(5) McNeill, V. F.; Loerting, T.; Geiger, F. M.; Trout, B. L.; Molina, M. J. *PNAS* **2006**, *103*, 9422.
(6) Huthwelker, T.; Ammann, M.; Peter, T. *Chem. Rev.* **2006**, *106*, 1375.
(7) Talukdar, R. K.; Burkholder, J. B.; Roberts, J. M.; Portmann, R. W.; Ravishankara, A. R. *J. Phys. Chem. A* **2012**, *116*, 6003.
(8) Walewski, Ł.; Forbert, H.; Marx, D. *ChemPhysChem* **2013**, *14*, 817.
(9) Walewski, Ł.; Forbert, H.; Marx, D. *J. Phys. Chem. Lett.* **2011**, *2*, 3069.
(10) Sugawara, S.; Yoshikawa, T.; Takayanagi, T.; Tachikawa, M. *Chem. Phys. Lett.* **2011**, *501*, 238.
(11) Takayanagi, T.; Takahashi, K.; Kakizaki, A.; Shiga, M.; Tachikawa, M. *Chem. Phys.* **2009**, *358*, 196.
(12) Gutberlet, A.; Schwaab, G.; Birer, Ö.; Masia, M.; Kaczmarek, A.; Forbert, H.; Havenith, M.; Marx, D. *Science* **2009**, *324*, 1545.
(13) Odde, S.; Mhin, B. J.; Lee, S.; Lee, H. M.; Kim, K. S. *J. Chem. Phys.* **2004**, *120*, 9524.
(14) Forbert, H.; Masia, M.; Kaczmarek-Kedziera, A.; Nair, N. N.; Marx, D. *J. Am. Chem. Soc.* **2011**, *133*, 4062.
(15) Leopold, K. R. *Annu. Rev. Phys. Chem.* **2011**, *62*, 327.
(16) Weimann, M.; Farnik, M.; Suhm, M. A. *Phys. Chem. Chem. Phys.* **2002**, *4*, 3933.
(17) Fárník, M.; Weimann, M.; Suhm, M. A. *J. Chem. Phys.* **2003**, *118*, 10120.
(18) Huneycutt, A. J.; Stickland, R. J.; Hellberg, F.; Saykally, R. J. *J. Chem. Phys.* **2003**, *118*, 1221.
(19) Ortlieb, M.; Birer, Ö.; Letzner, M.; Schwaab, G. W.; Havenith, M. *J. Phys. Chem. A* **2007**, *111*, 12192.
(20) Skvortsov, D.; Lee, S. J.; Choi, M. Y.; Vilesov, A. F. *J. Phys. Chem. A* **2009**, *113*, 7360.
(21) Zwier, T. S. *Science* **2009**, *324*, 1522.
(22) Flynn, S. D.; Skvortsov, D.; Morrison, A. M.; Liang, T.; Choi, M. Y.; Douberly, G. E.; Vilesov, A. F. *J. Phys. Chem. Lett.* **2010**, *1*, 2233.
(23) Morrison, A. M.; Flynn, S. D.; Liang, T.; Douberly, G. E. *J. Phys. Chem. A* **2010**, *114*, 8090.
(24) Letzner, M.; Gruen, S.; Habig, D.; Hanke, K.; Endres, T.; Nieto, P.; Schwaab, G.; Walewski, Ł.; Wollenhaupt, M.; Forbert, H.; Marx, D.; Havenith, M. *J. Chem. Phys.* **2013**, *139*.
(25) la Cour Jansen, T.; Knoester, J. *J. Chem. Phys.* **2006**, *124*.
(26) Masia, M.; Forbert, H.; Marx, D. *J. Phys. Chem. A* **2007**, *111*, 12181.
(27) Lin, W.; Paesani, F. *J. Phys. Chem. A* **2013**, *117*, 7131.
(28) Hassanali, A. A.; Cuny, J.; Ceriotti, M.; Pickard, C. J.; Parrinello, M. *J. Am. Chem. Soc.* **2012**, *134*, 8557.
(29) Lee, C.; Sosa, C.; Planas, M.; Novoa, J. J. *J. Chem. Phys.* **1996**, *104*, 7081.
(30) Bacelo, D. E.; Binning, R. C.; Ishikawa, Y. *J. Phys. Chem. A* **1999**, *103*, 4631.
(31) Milet, A.; Struniewicz, C.; Moszynski, R.; Wormer, P. E. S. *J. Chem. Phys.* **2001**, *115*, 349.
(32) Estrin, D. o. A.; Kohanoff, J.; Laria, D. H.; Weht, R. O. *Chem. Phys. Lett.* **1997**, *280*, 280.
(33) Chaban, G. M.; Gerber, R. B.; Janda, K. C. *J. Phys. Chem. A* **2001**, *105*, 8323.
(34) Daniel Boese, A.; Forbert, H.; Masia, M.; Tekin, A.; Marx, D.; Jansen, G. *Phys. Chem. Chem. Phys.* **2011**, *13*, 14550.

(35) Sillanpää, A.; Laasonen, K. *ChemPhysChem* **2005**, *6*, 1879.
(36) Ndongmouo, U. F. T.; Lee, M. S.; Rousseau, R.; Baletto, F.; Scandolo, S. *J. Phys. Chem. A* **2007**, *111*, 12810.
(37) Re, S.; Osamura, Y.; Suzuki, Y.; Schaefer, H. F. *J. Chem. Phys.* **1998**, *109*, 973.
(38) Devlin, J. P.; Uras, N.; Sadlej, J.; Buch, V. *Nature* **2002**, *417*, 269.
(39) Planas, M.; Lee, C.; Novoa, J. J. *J. Phys. Chem.* **1996**, *100*, 16495.
(40) Mancini, J. S.; Bowman, J. M. *J. Chem. Phys.* **2013**, *138*.
(41) Mancini, J. S.; Samanta, A. K.; Bowman, J. M.; Reisler, H. *J. Phys. Chem. A* **2014**, *118*, 8402.
(42) Mancini, J. S.; Bowman, J. M. *J. Phys. Chem. A* **2014**, *118*, 7367.
(43) Mancini, J. S.; Bowman, J. M. *J. Phys. Chem. Lett.* **2014**, *5*, 2247.
(44) Samanta, A. K.; Czakó, G.; Wang, Y.; Mancini, J. S.; Bowman, J. M.; Reisler, H. *Acc. Chem. Res.* **2014**, *47*, 2700.
(45) Knizia, G.; Adler, T. B.; Werner, H.-J. *J. Chem. Phys.* **2009**, *130*.
(46) Zhao, Y.; Truhlar, D. *Theor. Chem. Acc.* **2008**, *120*, 215.
(47) Paesani, F.; Xantheas, S. S.; Voth, G. A. *J. Phys. Chem. B* **2009**, *113*, 13118.
(48) Bakker, H. J.; Skinner, J. L. *Chem. Rev.* **2009**, *110*, 1498.
(49) Nibbering, E. T. J.; Elsaesser, T. *Chem. Rev.* **2004**, *104*, 1887.
(50) Li, H.; Blinov, N.; Roy, P.-N.; Le Roy, R. J. *J. Chem. Phys.* **2009**, *130*, 144305.
(51) Li, H.; Ma, Y.-T. *J. Chem. Phys.* **2012**, *137*.
(52) Colbert, D. T.; Miller, W. H. *J. Chem. Phys.* **1992**, *96*, 1982.
(53) Light, J. C.; Hamilton, I. P.; Lill, J. V. *J. Chem. Phys.* **1985**, *82*, 1400.
(54) Coxon, J. A.; Hajigeorgiou, P. G. *J. Mol. Spectrosc.* **2000**, *203*, 49.
(55) Faruk, N.; Schmidt, M.; Li, H.; Le Roy, R. J.; Roy, P.-N. *J. Chem. Phys.* **2014**, *141*.
(56) Eichenauer, D.; Le Roy, R. *Phys. Rev. Lett.* **1986**, *57*, 2920.
(57) Eichenauer, D.; Le Roy, R. J. *J. Chem. Phys.* **1988**, *88*, 2898.
(58) Kmetic, M. A.; LeRoy, R. J. *J. Chem. Phys.* **1991**, *95*, 6271.
(59) Blume, D.; Lewerenz, M.; Huisken, F.; Kaloudis, M. *J. Chem. Phys.* **1996**, *105*, 8666.
(60) Le Roy, R. J.; Davies, M. R.; Lam, M. E. *J. Phys. Chem.* **1991**, *95*, 2167.
(61) Kubo, R. In *Adv. Chem. Phys.*; John Wiley & Sons, Inc.: 2007, p 101.
(62) Skinner, J. L. *Mol. Phys.* **2008**, *106*, 2245.
(63) Cho, M. *Chem. Rev.* **2008**, *108*, 1331.
(64) Mukamel, S. *Principles of Nonlinear Optical Spectroscopy*; Oxford: London, 1995.
(65) Kwac, K.; Lee, H.; Cho, M. *J. Chem. Phys.* **2004**, *120*, 1477.
(66) Becke, A. D. *Phys. Rev. A* **1988**, *38*, 3098.
(67) Lee, C.; Yang, W.; Parr, R. G. *Phys. Rev. B* **1988**, *37*, 785.
(68) Grimme, S. *J. Comput. Chem.* **2006**, *27*, 1787.
(69) Troullier, N.; Martins, J. L. *Phys. Rev. B* **1991**, *43*, 1993.
(70) Barnett, R. N.; Landman, U. *Phys. Rev. B* **1993**, *48*, 2081.
(71) Martyna, G. J.; Klein, M. L.; Tuckerman, M. *J. Chem. Phys.* **1992**, *97*, 2635.
(72) Martyna, G. J.; Tuckerman, M. E. *J. Chem. Phys.* **1999**, *110*, 2810.
(73) Ramírez, R.; López-Ciudad, T.; Kumar P, P.; Marx, D. *J. Chem. Phys.* **2004**, *121*, 3973.
(74) Garcia-Viloca, M.; Nam, K.; Alhambra, C.; Gao, J. *J. Phys. Chem. B* **2004**, *108*, 13501.